A Review on Miniaturized Ultrasonic Wireless Power Transfer to Implantable Medical Devices

**RAJESH V. TAALLA, MD. SHAMSUL AREFIN, AKIF KAYNAK,
AND ABBAS Z. KOUZANI**, (Member, IEEE)
School of Engineering, Deakin University, Geelong, VIC 3216, Australia

Corresponding author: Abbas Z. Kouzani (abbas.kouzani@deakin.edu.au)

ABSTRACT Wireless power transfer has experienced a rapid growth in recent years due to the need for miniature medical devices with prolonged operation lifetime. The current implants utilize onboard batteries as their main source of power. The use of batteries is not, however, ideal because they have constrained lifetime requiring periodic replacement. Energy can be supplied to the implantable devices through wireless power transfer approaches including inductive, ultrasonic, radio frequency, and heat. The implantable devices driven by energy harvesters can operate continuously, offering ease of use and maintenance. Inductive coupling is a conventional approach for the transmission of power to implantable devices. However, the inductive coupling approach is affected by tissue absorption losses inside the human body. To power implantable devices such as neural, cochlear, and artificial heart devices, the inductive coupling approach is being used. On the other hand, ultrasonic is an emerging approach for the transmission of power to implantable devices. The enhanced efficiency and low propagation loss make ultrasonic wireless power transfer an attractive approach for use with implantable devices. This paper presents a study on the inductive and ultrasonic wireless power transfer techniques used to power implantable devices. The inductive and ultrasonic techniques are analyzed from their sizes, operating distance, power transfer efficiency, output power, and overall system efficiency standpoints. The inductive coupling approach can deliver more power with higher efficiency compared to the ultrasonic technique. On the other hand, the ultrasonic technique can transmit power to longer distances. The advantages and disadvantages of both techniques as well as the challenges to implement them are discussed.

INDEX TERMS Energy harvesting, implantable devices, wireless power transfer, inductive, ultrasonic, power transmission efficiency.

I. INTRODUCTION

Implants are medical devices that replace missing body parts, provide support to organs and tissues, and monitor and enhance biological/physiological parameters within the body [1]. They can be classified into two groups: active and passive. Active implants are devices that require an energy source to function, such as cardiac stimulators, neuro stimulators, drug pumps and cochlear implants. On the other hand, passive implants are devices that do not require an energy source to function such as orthopedic, cardiovascular stents, neurovascular clips and disks. Active implants may consist of power management, micro-controller, sensors, amplifiers and transceiver. On the other hand, passive implants may contain screws, rods, plates and disks. This paper focuses on active

implants because they facilitate continuous monitoring, diagnosing and closed-loop therapy [2], [3].

The method of capturing energy from energy sources around a device [4], [5] is referred to as energy harvesting. Implantable devices are usually powered by on-board batteries. Static energy-density, shorter lifespan, and larger size are among the drawbacks of batteries. Accordingly, several methods can be used to gather energy for powering implants [6], [7]. Devices driven by energy harvesters have extensive operation life-span and offer additional ease of use and maintenance [8]. Fig. 1 shows different types of energy harvesters including kinetic, thermal, solar, infrared radiant energy, and wireless energy transfer (capacitive coupling, inductive coupling, ultrasonic, EM radiative power) [4]–[8].
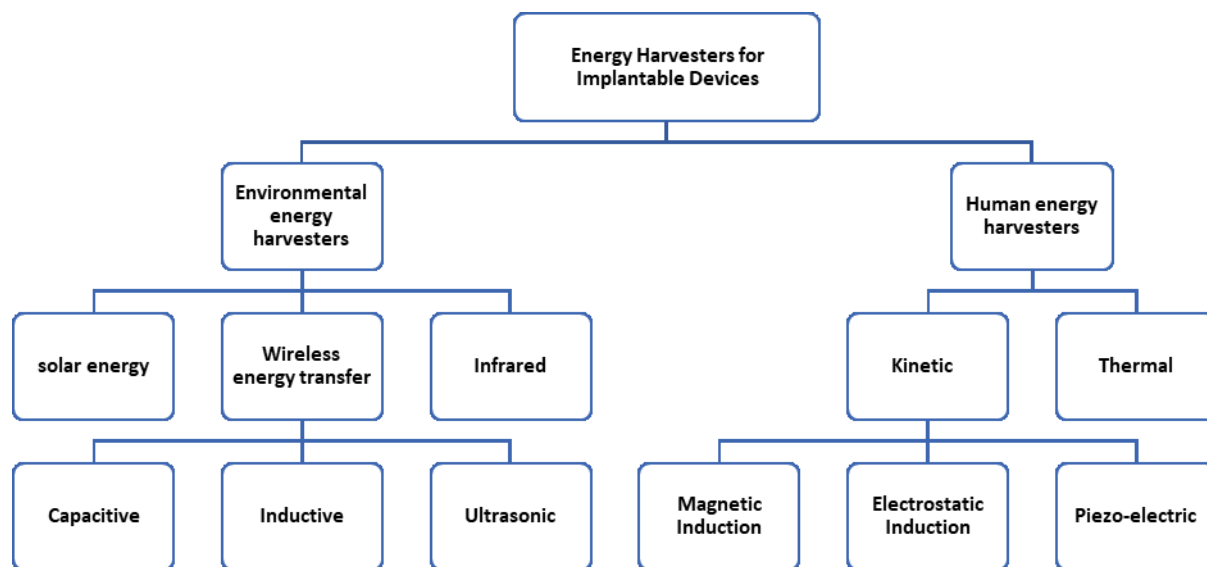
FIGURE 1. Different types of energy harvesters.

Kinetic and thermal energy harvesters are used to supply power to wearable and wireless implantable devices. Kinetic energy harvesters convert human motions into electrical energy. They consist of three types: piezoelectric, electrostatic and magnetic [5]. An impending limitation of kinetic energy harvesters is that they generate inadequate power, and only to people who have free movement of their body parts. Also, they usually have a large size. The developments and drawbacks of kinetic energy harvesters are described in [4] and [5]. The first energy harvesting device for human walking was fabricated in the Media Lab at Massachusetts Institute of Technology (MIT) [4]. The prototype developed by Shenck and Paradiso [9], produces 8.3 mW of output power, but it is useful for people who can walk normally.

Thermal energy harvesters exploit thermal gradients to produce energy based on differences in temperature. The power range of thermal energy harvesters when exploiting thermal gradients in the human body is low and not more than 100 μW [4], [10]. The developments and drawbacks of thermal energy harvesters are explained in [4] and [5]. Stark and Stordeur [11] attained 1.5 μW power for a 0.19 cm device with 5 K thermal gradient. Strasser *et al.* [12] obtained 1 μW with 1 cm area device and a 5 K thermal gradient. Cadei *et al.* [13] published a comprehensive review on kinetic and thermal energy harvesting technologies stating the power levels between 6 nW and 7.2 mW produced by energy harvesters.

Environmental energy harvesters are mainly of three types: solar, infrared, and WPT. The method of capturing energy from environment around a device [4], [5] is known as environmental energy harvesting. Solar energy harvesters can supply power to implants used by people who suffer from a problem in the movement of their body parts. The solar energy can vary due to the blocking of the light by

various obstacles. The major drawbacks in this approach is that the light does not penetrate into the body, and also some tags need to be placed under clothing [14], [15]. For powering large implantable devices such as brain and cardiac pacemakers, infrared radiation (IR) energy harvesters use an exterior infrared source [5]. These energy harvesters are not suitable for powering implants due to their low level of harvested energy, larger size, and operation complication with tissues of higher thickness [4], [5]. Some examples of IR energy harvesters are discussed in [16]. The primary element in IR devices is the implanted photodiode array. As an example, an IR emitter driven with 2.8 direct-current voltage, generates 4 mW of power. The temperature of the skin was increased by 1.4°C with the transmitted power, which might be an issue for soft tissues [4].

A WPT system typically consists of a transmitter (Tx) and a receiver (Rx), while the former is placed outside and later is located inside the human body. A WPT system can supply power to implantable devices to avoid the issue of toxicities caused by power/signal wires [17]. Impediments of wires are frequently documented in deep brain stimulation devices [18] as well as pacemakers and cardiac defibrillators [19]. Thus far, WPT is of four types: inductive, capacitive, microwave, and ultrasonic [5], [20]. Among these, the inductive WPT is widely used [5]. Powering of implantable devices wirelessly is normally attained through inductive links with low-frequency [20], as magnetic fields can penetrate well into body at lower frequencies. The power transmission efficiency of inductive links is very high [5]. One major downside of inductive links is their small transmission distance, and also significant drop in power transmission efficiency (PTE), while the Tx and Rx coils are not well aligned [21].

Capacitive WPT, on the other hand, is in its earlier stage of research and development. It is used for short-distance

transmission of power and data. For small distances, capacitive WPT achieves higher power transfer with reasonable efficiency [5]. The foremost drawback of capacitive WPT is that the tissue temperature may increase with plates, causing discomfort to patients [4]. The examples of capacitive WPT are discussed in [22]. Microwave WPT can provide very high efficiency and a wide propagation area [21]. It can achieve efficiency of up-to 80–90%. The drawback of microwave WPT is that, it suffers from microwave radiation that is unsafe [23].

Ultrasonic WPT, unlike the other WPT types, transfers power by propagating energy as sound or vibration waves. It has the advantage of deeper penetration depths. It can also travel through electrically conductive materials, which would be opaque to electromagnetic energy. It does not cause any harms to the human body, nor create EM interference [23].

This paper presents a description of the existing inductive and ultrasonic energy harvesting technologies for low power implantable devices. The paper is structured as follows. The inductive approach and the existing inductive energy harvesting technologies are discussed in Section II. The ultrasonic approach and the existing ultrasonic energy harvesting technologies are discussed in Section III. Section IV presents an analysis of the key aspects of the explored energy harvesters. The conclusions of this review together with future directions of this field are presented in Section V.

II. INDUCTIVE WPT

Inductive powering is used for powering implantable devices wirelessly at low frequencies, as magnetic fields can penetrate well into the body at low frequencies. For inductive links, the power transmission efficiency is very high. This section describes the principle of operation, advancements in inductive WPT, and existing challenges of inductive WPT.

A. PRINCIPLE OF OPERATION

The basic block diagram of an inductively coupled (IC) WPT is presented in Fig. 2. Inductive coupling comprises of two coils namely L1 and L2. The primary coil L1 is close to the skin and energized by sinusoidal current which generates alternating magnetic flux. This flux penetrates the turns of the implanted secondary coil L2 creating a voltage across it due to electromagnetic induction, which is then provided to the load (implanted device). The maximum voltage gain and therefore efficiency of the inductive link is achieved when both sides are tuned at the resonant frequency [5], [24].

IC is well suitable for implantable devices because the sensor is placed inside the body, and the control device is placed outside the body, and bidirectional communication can be performed [5]. One downside of IC is that the distance of transmission is very short. Furthermore, the power transfer efficiency significantly drops, when the transmitter and receiver coils are not well aligned. Regardless of these drawbacks, inductive WPT is often used due to its simplicity and good safety [21], [24].
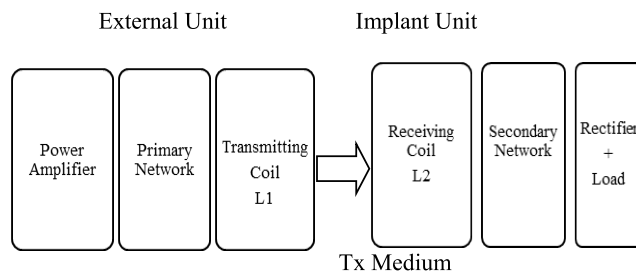
FIGURE 2. Inductive wireless power transmission network.

B. ADVANCEMENTS IN INDUCTIVE WPT

A frequency-shift keying (FSK) modulation with a class-E power oscillator was used by Troyk and DeMichele [25], in which an efficient power transmitter was combined with a high-speed data link. In this technique, continuous power transfer was combined with rapid data modulation to allow the transmitter current to be turned-on for as little as one cycle or turned-off for an arbitrary period.

A low power, high data rate demodulator such as binary phase-shift keying (BPSK) was established on a topology known as COSTAS loop, developed by Hu and Sawan [26]. The outcomes of this technique demonstrate that with 1.8 V of supply voltage and 0.7 mW of power, information could be carried at a rate of 1.12 Mbps. However, the complexity of the design was the major disadvantage of the BPSK demodulators based on COSTAS loop. Furthermore, the entire implanted system showed improvements in the observability and controllability by using BPSK demodulation along with a passive modulation. This technique permitted full duplex communication of data between an implantable device and an external controller.

Wang *et al.* [27] showed an adaptable inductive power telemetry intended for retinal prosthesis with 1 MHz and 20 MHz frequency carriers for power and data. At a separation of between 7 mm to 1.5 cm, this model delivered up to 250 mW of power. The power transfer efficiency was 30% at 7 mm. From the implant unit to the external unit, the information was transmitted at 3.3 kbps with a bit error rate (BER) of less than 10^{-5} by using a back-telemetry link. To encourage back data transmission alongside forward transmission of power, a pseudo pulse-width modulation was used in this system. The results showed that data transmission could be achieved without compromising the power transfer efficiency.

An interesting technique for visual prostheses and cochlear implants was discussed in [28], in which multiple carrier signals were used for effective wide band transmission of data and power over a wireless-connection. Both the experimental and simulation results showed that multiple carrier signals were feasible for transmission of data and power simultaneously. New alignments and geometries of coil implementation resulted in enhancement of required direct-coupling within the pairs of data or power, whereas unwanted cross coupling reduced among the pairs to lessen intervention between power and data carriers.

Lu and Sawan [29] used offset quadrature phase-shift key-ing (OQPSK) modulation structure because of its high data rate and effective bandwidth. The results revealed that the system exhibited low power and low area, 8 Mbps of data transmission rate with a frequency of 13.56 MHz and was easier to implement. The circuits were implemented with 1.8 V of supply voltages, consuming 16 μW of power for the modulator and 680 μW for the demodulator, respectively. The layout area of the modulator was only 0.185 mm×0.168 mm. For the suggested two demodulators, offset quadrature phase-shift keying had the same layout area of 0.61 mm × 0.39 mm, respectively. Demodulator-1 contained an input comparator whereas demodulator-2 did not have one.

Mandal and Sarpeshkar [30] used an impedance modulation technique in the uplink direction for transmission of information at a high bandwidth that reduced power in the implant unit - 2.8 Mbps at a BER of 10^{-6}, and 4.0 Mbps at a BER of 10^{-3}. In the downlink direction, 300 kbps of data was transferred as observed in experimental results. A 2 MW of power was dissipated by an external system and only 100 μW of power was dissipated by an internal system in the downlink. The other advantages of this technique included lower BER, exceptionally lower consumption of power by the internal unit and a very high data rate.

In [31], for maximizing the link efficiency of the inductive link, design procedures and optimization processes at lower coupling rates were proposed. Both the simulation and experimental results showed that output power of 100 mW was achieved at 2.5 MHz. The proposed method transferred data at a rate of 128 kbps with a link efficiency of 40%.

Silay *et al.* [32] proposed a novel method for cortical implants i.e., the concept of bio-compatible packing employing a matching network in between a rectifier and an inductive link. A 10 MW of power was delivered by a rectifier with 8.1% of power transfer efficiency and only 4.5% without a matching network. An efficiency of 8.3% with a matching network was attained, which is 2.4 times more than a system efficiency that does not contain a matching network. For 1 mW consumption of power at the load, there was an increase in efficiency by 5.8 times that of the link without a matching network. From this analysis, the authors stated that the PTE of the system could be increased with the help of a matching network.

Cartaa *et al.* [33] proposed a circuit that was operated at a frequency of 1 MHz and 50% of the entire efficiency was achieved at 1 cm separation, and 380 mW of output power was delivered to observe the parameters of circuits that allowed devices to increase separations up-to 5 cm and minor coil misalignments using the absorption modulation technique. This technique revealed that the implemented tuning strategy increased the power transmitted by two factors. The increased efficiency of the system was proven by retaining the secondary energy level constant by way of combined smart regulation of power and tuning.

To improve the PTE of a structure, Kiani *et al.* [34] proposed a 4-coil inductive link. Both simulations and

measurements results were verified. The authors stated several design examples for 12 cm separation and 13.56 MHz carrier frequency of different inductive links such as 2-, 3-, and 4-coils. The results showed PTE of 15% for 2-coil, 37% for 3-coil, and 35% for 4-coil, respectively. The PTE and power delivered to load (PDL) introduced in this system was significantly improved at large coupling distances. The suggested 3-coil power delivered to load was one and a half times more than the 2-coil and 59 times more than the 4-coil links at 12 cm.

WPT based on resonance type was proposed in [35] for efficient transfer of power over long distances. Four-coil inductive links were used instead of 2-coil inductive links in this method. With the help of high-quality coils, the system efficiency was improved and the effects of low-coupling coefficient between the coils were compensated for in the 4-coil design. In this system, at a separation of 10 mm to 20 mm, 700 kHz frequency was used. When compared with the 2-coil system, the resonance-based wireless power delivery system showed 80% of PTE. A PTE of 82% was obtained at 20 mm and dropped to 72% at a separation of 32 mm. The results showed that a 4-coil link is robust and efficient for long ranges.

In [36], an efficiency of 24.6% was achieved at a load of 10 mW by using a novel packaging topology occupying a small area implanted in a cranial bone, consisting of a readout part and a transceiver part. For supplying power to the implant and achieving external reader communication, the fixed transceiver was used. For neural activity recording, the movable readout part was used. For power and information transferring, these two parts were attached to a flexible cable. The transceiver part was made-up of bio-compatible silicone elastomer and covered with Parylene-C.

Duan and Guo [37] presented a new technique for the optimization and characterization of rectangular coils commonly used in inductively coupled systems. In this study two rectangular coils were designed and achieved a PTE of 46.4% at 3 MHz frequency and a separation of 10 mm. The proposed technique was tested through simulations and measurements.

Kiani and Ghovanloo [38] suggested a novel figure-of-merit (FoM), which incorporated both PTE and PDL with correct masses to exhibit an equilibrium at the same time between high PTE and PDL. Their outcomes demonstrated that the FoM accomplished 1.65× greater PTE for an optimized inductive link compared to PDL, i.e., 72.5% vs 44% and achieved PDL 20.8 times larger than the optimized PTE i.e., 177 mW vs 8.5 mW. When optimized FoM was compared with the PTE and PDL, there was 24% higher power transfer efficiency and power delivered to load for the optimized inductive links. The accuracy of the procedure for the theoretical design is supported by the measured results.

In [39], for cortical implants, a closed-loop wireless powering link was introduced. When the implant was placed in vitro, the efficiency dropped from 54.8% to 47.2% at a separation distance of 10 mm and as the distance increased to 13.5 mm, the efficiency dropped to 32.5%.

For a 10-mW rectifier load, 18.5% of power transfer efficiency was measured at 8 MHz. The measured PTE's were 4.4% and 17.9% for the least power consumption (1 mW), and most power consumption (20mW), respectively. For a 10- mW load at a 13.5 mm separation distance, the system had 10.6% of power transfer efficiency.

Keikhosravy *et al.* [40] presented an inductive coupling system for monitoring wireless implants on the 0.13-μm CMOS technology with very low power consumption. The re-narrowing of blood vessels at the site of a smart stent was monitored by the presented design. The rectifier in this system offered two optimal efficiency power points for two different modes of operation, such as monitoring and alignment modes. The simulation outcomes for the alignment and monitoring circuits of the system were as follows: for the rectifier with input power of 10.36 dBm, the PCE was 53% and for 4.06 dBm, the PCE showed 62%. For 0.6 V supply voltage, 12 μA was consumed by the alignment unit and only 176 μW was consumed by the monitoring unit.

RamRakhyani and Lazzi [41] introduced a new telemetry system for transfer of data and power over an inductive link, based on multi-coil, and compared this technology with a 2-coil equivalent system. A two-port model and a network theory were used by the multi-coil system. The examination of the two-loop and the multi-coil, e.g. 3-coil and 4-coil system, demonstrates that the multi-coil system could be utilized viably to enhance the PTE and data transmission. One substantial benefit of the 3-coil structure was that it provided an alternative non-surgical, cost-effective high-performance solution that could be utilized to redesign 2-loop frameworks already implanted in patients with no prerequisite to adjust the implanted coil. Moreover, the results based on simulation were almost equal to the results obtained from experiment.

A wireless powering implantable heart monitoring system for freely moving animals was introduced in [42]. The implanted sensor measured the left ventricular blood pressure and sent the information to the external unit for animal monitoring. By using the magnetically coupled coils, wireless power transmission was performed at 8 MHz at 25 mm separation. By using the on-off keying (OOK) modulated transmitter, data transmission was achieved at 868 MHz. The overall implant unit size was 26 mm × 13 mm × 5.5 mm, and 7 mW consumption of power.

The results of a resonance built multi-coil for an implant system [43] are as follows: at 1cm distance and 3.87 W of PDL, the PTE of 83.3% was obtained in a 3-coil system; at 4 cm separation and 115 mW of PDL, the PTE of 76% was observed in a 4-coil system.

Kava *et al.* [44] reported the design of a 2-coil system for transfer of power to a batter implant without causing damage to tissue. In this design, different signals with a frequency of 575 KHz and 700 KHz, were used to transfer power in the 2-coil system. The diameters of the primary coil and the implanted coil were 68 mm and 18 mm, respectively, at 10 mm to 50 mm. The results attained were better when compared with the conventional 2-coil system with an efficiency of higher than 40% at 30 mm distance.

An inductive power transfer system containing a 20 mm × 20 mm flexible 8-layer receiver coil with a PTE of 40% for intractable epilepsy treatment on 0.13-μm CMOS neuro stimulator was presented in [45]. The total dissipation of power with and without FSK transmission was 5.78 mW and 2.17 mW, respectively.

To use in freely moving animal experiments, Xu *et al.* [46] proposed new wireless power and data transmission based on an inductive link with a low-cost and programmable epidural spinal cord stimulation (ESCS) system. Specifically, this framework was intended to research the neural component of merging ESCS with partial weight-bearing therapy (PWBT) to enhance locomotive act after spinal cord injury (SCI).

A class-D power amplifier (PA) that interfaced with numerous implant units for epidural incitement was presented in [47]. The measured outcomes from the chip fabricated models demonstrated great performance based on simulation. The efficiency of the amplifier was measured to be greater than 80% at optimal dead-time. The power amplifier could deliver power of more than 30 W towards a 5 Ω load, when working with a supply of 30 V.

Ibrahim and Kiani [48] studied viability of using printed spiral coils (PSCs) at different peak frequencies with higher PTE for powering mm-sized implants. To power 1 mm diameter of an implant positioned 10mm deeper in tissue, the dimensions of transmit and receive printed spiral coils were verified at frequencies of 50 MHz, 200 MHz, and 500 MHz. At optimal frequencies of 50 MHz and 100 MHz, in simulations, 0.13% and 3.3% of maximum PTE were achieved, and the power delivered was 65.7 μW and 720 μW under the constraints of a specific absorption rate, respectively.

Soltani *et al.* [49] presented a methodology for wireless chronic rodent electrophysiology applications based on design considerations of an inductive coil. On activation of the transmitter coil, this structure discovered the vicinity of the receiver. This method used 1.5 MHz frequency of operation and delivered maximum power to load of 15.9 W. At a separation distance of 8 cm, 39% of PTE was attained and 13% at a separation distance of 11 cm.

For inductive WPT, maximum power of 15.9 W was achieved at a separation distance of 8 cm with an efficiency of 39% [49]. The maximum efficiency of 76% was achieved at 4 cm distance with an output power of 115 mW in inductive WPT [43]. The minimum efficiency of 0.13% was achieved at 1 cm with an output power of 65.7 μW and frequency of operation is 50 MHz [48].

C. EXISTING CHALLENGES OF INDUCTIVE WPT

Several constraints exist in developing inductive WPT frameworks, such as: frequency of operation, PTE, system efficiency, output power level, power factor, maximum output current and output voltage, temperature, weight and volume,
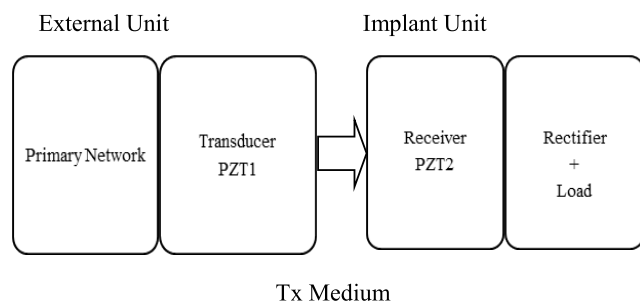
FIGURE 3. Ultrasonic wireless power transmission network.

passive or active, protecting, level of resistance in both the vertical (z) parallel (x, y) planes, and so on. For inductive WPT, efficiency is the most important parameter in most cases. For large primary sources, the power transmission can be increased [50].

D. SUMMARY

The inductive WPT technique uses different modulation methods, for example offset quadrature phase-shift keying, pulse-position modulation, amplitude-shift keying, absorption, frequency-shift keying, impedance, quadrature phase-shift keying, on-off keying, passive phase-shift keying, phase-shift keying and quadrature. These techniques use different methods like 1-coil, 2-coil, 3-coil, 4-coil and multi-coil. The inductive WPT technique produces power between 22.7 μW and 15.9 W, and the minimum and maximum efficiencies of 0.15% to 76%, respectively. The maximum separation distance has been 20 cm [51]. The frequencies of operation have been between 25.5 kHz and 460 MHz.

III. ULTRASONIC WPT

The ultrasonic WPT operation is established from vibration or sound waves with the help of piezoelectric transducers. The word ultrasonic refers to the frequency beyond the audible range greater than 20 kHz. The ultrasonic WPT technique has the advantages of greater penetration depths and shorter wavelengths and can also travel through electrically conductive materials which are opaque to electromagnetic energy. The ultrasonic WPT technique does not cause harm to the human body and creates no electromagnetic (EM) interference.

A. PRINCIPLE OF OPERATION

An ultrasonic WPT system contains both external and implant units with piezoelectric transducers on either side and separated by a medium of transmission as presented in Fig. 2.

Energy transfer through the skin requires an external transducer (transmitter) attached to the skin surface and facing an implanted transducer (receiver). An electrical power source energizes the transmitter that converts the electrical energy into ultrasonic waves. These ultrasonic waves carry the energy through the tissue toward an implanted receiver positioned within the radiation lobe of the transmitter.

The piezoelectric receiver converts the ultrasonic energy back into electrical energy and a low-loss rectifier network rectifies and filters the output voltage of the receiving transducer, while reflecting an impedance conjugate toward input terminals of the piezoelectric element. To minimize the inconvenience caused to the patient as well as to ensure a close fit to the body, the device should be lightweight and thin.

B. ADVANCEMENTS IN ULTRASONIC WPT

Kawanabe *et al.* [52] and Suzuki *et al.* [53] reported two crucial works on ultrasonic projection. In these works, they showed that ultrasonic energy transfer is a highly suitable method for in-body implants. The optimal frequency of 1 MHz was used for resonance power supply and 2.1 W of maximum output power and 20% of efficiency were achieved at a 30 mm separation distance for both systems.

Suzuki *et al.* [54] presented a new way of supplying electric power to implanted biomedical devices. Their system was non-invasive and used two kinds of energy, magnetic and ultrasonic. It could provide high power levels harmlessly. The energies were obtained by two types of vibrators, i.e., piezo and magneto striction devices. The internal and external magneto striction devices were set up and biased by a permanent magnet to operate optimally. The system was investigated at two resonance frequencies, 50 kHz and 100 kHz. At 50 kHz, the maximum output power (4.0 W at 60 Ω) was less than the output of the transformer (15.0 W at 30 Ω). The experiments showed that the hybrid power supply system (HPSS) could transmit more power than a conventional transformer system at high frequencies and large load resistances. The HPSS output (5.4 W at 200 Ω) was larger than the transformer output (4.6 W at 70 Ω) at 100 kHz. The power was 1.5 times greater than that of the 50 kHz transformer and the same result applied for the power per unit weight. Although the efficiency of the 100 kHz HPSS was 36%, the same was also true for the 100 kHz transformer.

For powering a battery free implant, Arra *et al.* [55] proposed a new method based on ultrasonic WPT. The power and data link concept were constructed using piezo-electric crystals. The experiments took place in degassed water demonstrating the possibility of an ultrasonic link. When the transmitter was driven with a power of 250 mW and increased by 0.1 mm steps of separation from the receiver, 21-35% efficiencies were achieved at separation distances between 5 mm and 105 mm.

Shigeta *et al.* [56] proposed an effective wireless transmission of power, based on ultrasonic topology. For realizing an efficient system, first, the input source, amplifier circuit, and transducer's impedance matching were considered. Also, the optimum position of the two transducers necessary for obtaining a high transmission efficiency in water was determined. Moreover, to achieve high direct current (DC) output voltage, a voltage booster circuit was designed. The distance between the two transducers, was about 70 mm. In the ultrasonic transmission experiment, the voltage necessary for operation of the in-vivo device was attained. Still, because the

transducers used in this experiment were designed for ultrasonic imaging applications, higher transmission efficiency of the electric power was not achieved.

An ultrasonic WPT system for an implantable biomedical device with fully packaged ultrasonic power receivers was designed by Shih and Shih [57]. To accomplish the best performance, 35 kHz of dominant frequency was selected. The proposed device could recharge a 25 μJ battery in a non-delivery mode in 18.1 minutes with 1.23 mW of power. To offer biocompatibility, cohesive gel was utilized as a packaging material. Furthermore, to abstract energy in the biotic environment, Young's modulus of the packaging material was guaranteed to be less than that of muscular tissue. For designing an antenna, a light-weight material, aluminum, was preferred. The cubic package was planned with the measurements of 10 mm $\times$ 10 mm $\times$ 5.5 mm, with 5 mm radius for spherical package.

Ozeri and Shmilovitz [58] presented the feasibility of ultrasonic WPT to transmit power of up to 100 mW at a separation distance of 40 mm. For this purpose, they designed a piezo transducer of circular shape with a 15 mm diameter and a thickness of 3 mm. In a lossy environment, and at an operating frequency of 673 kHz, a PTE of 27% was achieved with 94 mW/cm2 power-density. Moreover, a rectification efficiency of 88.5% was delivered by the receiver's power control unit.

Ozeri *et al.* [59] proposed an enhanced type of ultrasonic WPT model constructed with a Gaussian distribution on a kerfless transmitter. The link was fabricated with transducers in a flat, circular shape to employ Tx and Rx. The frequency of operation was modified to 650 kHz and the depth of penetration was improved from 40 mm to 50 mm. The power level was kept constant, but the dimensions of the device were changed to a diameter of 15 mm and a thickness of 5 mm. Better performances were attained with these modifications. For a 5 mm separation distance, the PTE was increased to 39.1% and at 40 mm the PTE was 17.6% with a power of 45 mW. Moreover, at the load side on the implant, the power rectification efficiency was also increased to 89%.

For in-situ oxygenation of tumors over simple water electrolysis, Maleki *et al.* [60] introduced an ultrasonically powered implantable micro device. The proposed device had less directionality at greater distances and smaller receiver dimensions, and the device delivered superior PTE's. The device could potentially be appropriate for intra-tumor supplements with a biopsy needle because of its small size i.e., 1.2 mm $\times$ 1.3 mm $\times$ 8 mm, which would permit numerous micro-devices for insertion. The outcomes of the in-vitro experiments demonstrated that the proposed model could produce greater than 150 μA through electrolytic disassociation of oxygen measuring 0.525 μL/min.

Shigeta *et al.* [61] presented a fundamental Mason's equivalent circuit based on the power transfer technique by using a commercial transducer. A multi-physics stimulator, ANSYS, was used to model the transducer structure and materials. The outcomes of this technique confirmed that the PTE was radically enhanced from 1% to 60%. Moreover, the authors completed transducer designs and presented an overall system efficiency of over 50%.

A neural stimulator with only three discrete components was presented in capsule form by Larson and Towe [62]. This system basically worked at a lower duty-cycle and when stimulus was necessary, it released ultrasound. The capsule was 8 mm long and was intended to be gripped straight upon a fringe nerve. At 1 MHz frequency of operation, it could produce currents over 1 mA. The device was placed in the body of a rat for in-vivo testing and effectively exhibited the potential to harvest energy with an energy density of 10–150 mW/cm^2.

A tissue-mimicking phantom creating 0.5 dB/MHz/cm ultrasonic attenuation was used by Tsai *et al.* [63] during estimations. In this method, ASK, FSK, and PSK variations were tested and BERs were calculated to verify the diverse coding schemes. The transmitting transducer generated 112 mW of ultrasonic power, received and used 4.15 mW, of which only 1.8 mW of power was consumed for neural stimulation. A BER of 10^{-6} was accomplished as well as a 25 Kbps data rate. The power transmission of the existing device could be increased to 19.76 mW.

Sanni *et al.* [64] reported a multi-tiered interface for deeper implants to benefit from the collective arrangement of inductive and ultrasonic harvesting. The inductive portion of the system was designed with a 2 MHz carrier frequency along with a driver and envelope detector circuit. The piezo subsystem comprised a signal conditioner, a driver and power circuits. At 10 mm, the proposed system transferred 5 W of power with 83% of efficiency. However, at 70 mm in liquid environments, this system transferred only 29 μW of power with a 1% efficiency. The consumption of power for the entire system was 2.3 W. Mazzilli *et al.* [65] presented a new system of ultrasonic WPT for deeply implanted devices. The proposed system had a theoretical link efficiency of 10.6%.

Lee *et al.* [66] proposed a biocompatible transducer using the method of ultrasonic resonance. The diameters of the transducer and receiver were 50 mm. At penetration depths of 20 mm to 50 mm, the tests were conducted under two mediums, namely water and tissue. In water, at an operating frequency of 243 kHz, the efficiency of the transducer was 55% at 10 mm, and dropped to 35% as the distance increased to 100 mm. At an operating frequency of 290 kHz, in a tissue environment, the system showed an efficiency of 21% and 6.5% at depths of 23 mm and 34 mm, respectively. For a frequency of 250 kHz, the output power of 2.6 mW was acquired with an efficiency of 18%.

By using a 0.18-μm CMOS process, a front-end ultrasonic power link for implantable biomedical devices was presented in [67]. For attaining a high level of integration over PZT, the proposed system worked with a capacitive micro machined ultrasonic transducer (CMUT) that provided wider bandwidth and higher sensitivity. At a depth of 70 mm in tissue, 0.3% efficiency was attained over the entire power link, assuming a CMUT transducer efficiency of 76% and an attenuation

of 0.63 dB/cm over fat tissue. The projected ultrasonic link for receiver contained 380 kHz of capacitive micro machined ultrasonic transducer operating frequency. It accomplished 76% efficiency and acquired 3.896 μW of total power loss.

For implanted hearing aids, Leadbetter *et al.* [68] projected a power and signal delivery system. At 1.07 MHz frequency of operation, the prototype was verified in a liquid environment with a 950 Ω loaded transducer. By using this model, a better efficiency of 60% was offered which accounted for 45% of PTE. The high efficiency achieved with the relatively small transducers (1.2 mm by 5 mm) was promising for use with low power and low voltage implanted hearing aids. The use of composite piezoelectric provides thinner transducers than solid piezoelectric disks, further improving surgical placement options when device thickness is a concern.

Kim *et al.* [1] examined an electromechanical interrogation scheme for use in implants. The authors developed an implantable pressure sensing system driven by mechanical vibrations in the frequency of the noticeable ultrasonic range. This system improved the range of examination, eased the inductive powering issues caused by misalignment and the receiver circuitry was also simplified. A pressure sensitive inductor coil was used in the fabricated prototype and tested under in-vitro and in-vivo circumstances. The dimension of the prototype was 40 mm length, and 8mm diameter. At a separation distance of 15 cm, for transmission operation, the active resonant frequency of greater than 350 Hz was used. Moreover, for generation of 1 W/mm^2 output power, 11.7 W of power was consumed by the transducer. Still, 16 μW could be generated using 40 mm^2 active piezo area with a maximum efficiency of 1.4×10^{-7}.

Mazzilli *et al.* [69] attained a system efficiency of 2.3% at a distance of 105 mm for wireless power transmission without a load application, but the efficiency dropped below 1.6% when a phantom model was used. The active transducer area was defined as 30 mm $\times$ 96 mm for transmitting, and 5 mm $\times$ 10 mm for receiving and functioned with a frequency of 1 MHz.

An ultrasonic WPT using a piezoelectric composite transducer was presented by Lee *et al.* [70]. The structure was projected for use in powering a brain machine interface (BMI) system. For both transmit and receive, the resonance frequency was set to 250 kHz, whereas the measured frequency was about 280 kHz. From the tests, in water it was revealed that for 1 mm and 20 mm separations, efficiencies of 55% and 50% were achieved, respectively. In the case of animal tissue, 15.5 mW of applied input power was noted, and 2.6 mW of output power was achieved. Hence, at 18 mm, an efficiency of 18% was accomplished by the overall system.

For a non-invasive process, distances of 85 mm were attained by Shmilovitz *et al.* [71]. In this process, an inductive link was used to control the harvested power of an ultrasonic link. The ultrasonic WPT with 35 mW was designed using a 2-PZT with the same dimensions at 720 kHz vibration

frequency of operation. Only 50 μW of power was used by the circuitry of the implant, comprising the power used for excitation of the coil.

Fang *et al.* [72] examined the possibility of wireless transmission of energy to an implanted biomedical device with a receiver separation of more than 10 cm from the surface of the tissue. The use of a commercial off-the-shelf (COTS) 3.5 MHz diagnostic ultrasound device was opted. The work demonstrated the supply energy to a PZT transducer that was encapsulated using an interrogation protocol made of B-mode to recover the data from the transducer using a B-mode video sequence. The transducer of 0.6 mm thickness, area of 1.1 cm^2, and operating frequency of 3.4 MHz was used. From the interrogation results, it was observed that the highest recorded voltage was 5.7 V with a separation distance of 5 mm and a load of 10 Ω. However, the received power was reduced to less than 1 μW when a separation of 100 mm was applied.

Omnidirectional powering by ultrasonic wave was explored by Song *et al.* [73]. Frequencies of 1.15 MHz and 2.3 MHz were selected for operation of a transducer with a peak ultrasonic intensity of 720 mW/cm2. Receivers made of PZT with diverse sizes were validated for omni-directional capabilities. For 20 cm, different receiver sizes provided received power of 2.48 mW, 8.7 mW, and 12.0 mW from 1 mm $\times$ 5 mm $\times$ 1 mm, 2 mm $\times$ 2 mm $\times$ 2 mm, and 2 mm $\times$ 4 mm $\times$ 2 mm sized receivers, with efficiencies of 0.4%, 1.7% and 2.7%, respectively.

In [74], an ultrasonic demodulator with OOK/ASK was outlined. An OOK/ASK modulation was used to obtain a receiver with low-power, because this modulation scheme removed the need for a synthesizer or a local oscillator. The data signals were transmitted at 50 kbps over a down-link at 1 MHz. For a supply voltage of 1.5 V, 184 μW of power was consumed, that created an OOK/ASK demodulator apt for biomedical implantable devices with low power of operation.

Rosa and Yang [75] presented a wirelessly activated implantable device to enable ultrasound emissions for computing biological tissue parameters namely, bio-potentials, thermal gradients, pH, and a concentration of electrolytes. In active mode, the device worked with 0.8 V, and an overall current of 60 μA was consumed at 3 cm separation from the source, by a sinusoid of 400 kHz with 20 mW/cm^2 of power density. The outcome revealed that the analog modules of the sensor could be operated at larger separations, while the voltage of the harvester dropped lower than 0.5 V.

Vihvelin *et al.* [76] described a method for a typical ultrasonic separation by changing the transmit frequency in a ultrasonic WPT structure. Experiments were conducted using a fixed resistive load for simplicity. A porcine tissue sample of 5 mm was used to simulate in-situ implant circumstances. The system showed PTEs from 9% to 25%. With the help of an active frequency compensation method, the PTE could be increased within a range of 20-27%. The strategy of frequency compensation was low-power because it was only used for the transmitter side measurements

and required no communication between the external and implanted units, making it suitable for active implantable biomedical applications.

Chang *et al.* [77] presented a fully packed implant 30.5mm^3 in volume with bidirectional ultrasonic power and data links attaining 95 kbps with a BER of 10^{-4} at a depth of 8.5 cm and with 1mHz frequency of operation. The authors stated that they could accomplish greater than 10 cm depth with access to an external beam former. When compared with the previous stated ultrasonic powered implants, the proposed implantable device was 2.5 times smaller and penetrated two times deeper. Also, with inductively powered implants, the proposed implantable device was 10× smaller and 10× deeper.

Meng and Kiani [78] developed an ultrasonic link and optimized it for WPT to a 1 mm^3 implant. The implant was placed on a silicon die with a disk-shaped piezoelectric transducer. In simulation outcomes, at 1.8 MHz of carrier frequency and separation of 3 cm, 2.11% of PTE was attained for a 2.5 kΩ load resistance. To confirm the proposed technique, an ultrasonic link was established for a 1 mm^3 implant placed on a printed circuit board (PCB). It showed 0.65% of simulated PTE and 0.66% of measured PTE.

In another example, a maximum efficiency of 50% was achieved at an operating frequency of 1.2 MHz [61]. As the required active area was small, the separation distance was therefore relatively small, and a maximum separation distance of 400 mm was found. The efficiency of the device could reach up to 50–81% for the theoretical design, however, dropped to 45% for the practical implementation.

C. EXISTING CHALLENGES OF ULTRASONIC WPT

The ultrasonic WPT technique has several issues to be addressed as follows:

1) REFLECTIONS

A propagated sound wave is significantly affected by reflection and, hence, results in spatial resonance and energy loss. This issue is mainly significant for measurement of ultrasonic WPT, as it confines the optimum position of the transmitter and receiver. Therefore, optimal transducer arrangement needs to be selected.

2) EFFICIENCY

For implantable devices, the efficiency still lies within 45%. Again, the current generation value in the receiver side is very low compared to voltage generation. Hence, while a converter can use the total generated power, this requires extra circuitry which consequently increases the size of the device. However, efficiency can be increased by using guided sound waves which also confines the location of the transmitter and receiver.

3) HEATING

Heat generation in the devices is a challenge, yet the generated heat lies within a tolerable limit for low power applications.

4) EFFECTS OF PROLONGED EXPOSURE

It was predicted that long-term exposure to ultrasonic waves may cause damage to human tissue. Specifically, the cavitation effect affects skin cells [31]. The thermal effect, conversely, causes a temperature increment near, or at, the bones. The directed sound beam is the reason in both cases. Therefore, it is recommended to follow the safety regulatory instructions for ultrasound diagnostic devices.

D. SUMMARY

The ultrasonic WPT technique uses different types of transducers such as piezo-electric, PMN-PT, ceramic, etc., and different mediums like tissues, skin, air, water, nerves, etc. The ultrasonic WPT technique produces output power between 1 μW and 5.4W, and minimum and maximum efficiencies of 0.2% and 50%. The frequencies of operation are between 35 kHz and 30 MHz. For ultrasonic WPT, a maximum power of 5.4 W is reported with an efficiency of 36%, at a separation of 4 cm and an operating frequency of 100 kHz [54].

IV. COMPARISON AND DISCUSSION OF INDUCTIVE AND ULTRASONIC WPT

The key features of current inductive and ultrasonic WPT techniques have been summarized in Sections I and II. For each WPT approach, Tables 1-3 show the relevant references, frequency of operation, active range, efficiency and output power. Implantable devices typically need less power to operate, mostly in the mW range. Hence, most of the current works are focused on this power limit. The inductive WPT technique produces a power between 22.7 μW and 15.9 W, and minimum and maximum efficiencies of 0.15% to 76%, respectively. The maximum separation distance is 20 cm [51] with frequencies of operation between 25.5 kHz and 460 MHz.

Similarly, the ultrasonic WPT technique produces a power between 1 μW and 5.4 W, and minimum and maximum efficiencies of 0.2% and 50%, respectively. The frequencies of operation are between 35 kHz and 30 MHz. For the inductive WPT technique, a maximum power of 15.9 W was achieved at a separation distance of 8 cm with an efficiency of 39% [49]. The maximum efficiency of 76% was achieved at a 4 cm distance with an output power of 115 mW in [43]. The minimum efficiency of 0.13% was achieved at 1 cm with an output power of 65.7 μW and a frequency of operation of 50 MHz [48].

For the ultrasonic WPT technique, a maximum power of 5.4 W was obtained with an efficiency of 36%, at a separation of 4cm and an operating frequency of 100 kHz [54]. The maximum efficiency of 50% was achieved at an operating frequency of 1.2 MHz [61]. As the required active area to

TABLE 1. Existing inductive WPT works.

Reference	Frequency	Modulation/ Methodology	Data rate	Active Range	Efficiency	Output power
Lu and Sawan [29]	13.56MHz	OQPSK	8 Mbps	Not specified	Not specified	0.91mW
Mandal and Sarpeshkar [30]	25MHz	Impedance	2.8 Mbps	20mm	Not specified	2.5mW
Catra et al. [79]	10kHz	OOK & Absorption	4.8 kbps	100mm	Not specified	200mW
Low et al. [80]	134kHz	Not specified	Not specified	10mm	75.7	Not specified
Ali et al. [31]	2.5MHz	ASK	128 kbps	Not specified	40	100mW
Yu et al. [81]	25.5kHz	Not specified	Not specified	10mm	0.61	0.008W
Simard et al. [82]	13.56MHz	PSK	4.16 Mbps	5mm	9.5	Not specified
Silay et al. [83]	1MHz	Not specified	Not specified	10mm	14.85	Not specified
Carta et al. [33]	1MHz	Absorption	1-10 kbps	10mm	50	380mW
Kiani et al. [34]	13.56MHz	Not specified	Not specified	120mm	Not specified	43.4mW
Ram Rakhyani et al. [35]	700kHz	Not specified	Not specified	10-20mm	82	Not specified
Silay et al. [32]	8MHz	Not specified	Not specified	10mm	24.6	10mW
Kiani and Ghovanloo [38]	13.56MHz	Not specified	Not specified	Not specified	Not specified	177mW
Adeeb et al. [84]	200kHz	FSK	10 kbps	10-40mm	12.5	125mW
Silay et al. [39]	8MHz	Not specified	Not specified	10mm	10.6	10mW
Keikhosravy et al. [40]	6.8MHz	Not specified	Not specified	30-40mm	Not specified	176µW
Kilinc et al. [42]	8MHz	OOK	125 ps	25mm	Not specified	7mW
Kilinc et al. [85]	13.56MHz	ASK	Not specified	30mm	Not specified	2mW
Kilinc et al. [86]	13.56MHz	PPM	5.55 kbps	30mm	21	22.7µW
Mirbozorgi et al. [43]	13.56MHz	Not specified	Not specified	40mm	76	115mW
Kiani et al. [87]	2MHz	QM	Not specified	80mm	27	1.45W
Kava et al. [44]	700kHz	2-coil system	Not specified	30mm	40	Not specified
Zargham and Gulak [88]	100-250MHz	Not specified	Not specified	10mm	0.8	Not specified
Ibrahim and Kiani [89]	20MHz	Not specified	Not specified	10mm	1.4	2.2mW
Ibrahim and Kiani [48]	50MHz	Resonant	Not specified	10mm	0.13	65.7µW
Soltani et al. [49]	1.5MHz	Not specified	Not specified	80mm	39	15.9W
Ahn and Ghovanloo [90]	200MHz	Not specified	Not specified	12mm	0.56	224µW
Gougheri and Kiani [91]	40MHz	Not specified	Not specified	70mm	2.56	Not specified
Gougheri and Kiani [92]	100MHz	Optimal wireless receiver	Not specified	20mm	Not specified	Not specified
Zhao et al. [51]	460MHz	Multi-coil array	Not specified	200mm	0.66	Not specified
Gougheri and Kiani [93]	1MHz	Adaptive Reconfigurable voltage/current mode power management	Not specified	60-135mm	Not specified	Not specified
Pan et al. [94]	10.4-13.56MHz	Not specified	Not specified	42mm	>35	18mW
Jiang et al. [95]	13.56MHz	PPSK	1.35 Mbps	5-15mm	Not specified	<100mW

propagate energy is small, the separation distance is therefore relatively small, and a maximum separation distance of 400 mm was found. The efficiency of the devices could reach up to 50–81% for theoretical designs, however, dropped to 45% for practical implementations.

For implants, the receiver device needs to be as tiny as possible - smaller than 10 mm^2 is a preferable size. Different frequency ranges were used to design the previously proposed

ultrasonic WPT based on the type of applications. Naturally, intermediate frequencies were used for implant systems. The preferable frequency range for implants is 1.3 MHz and below.

The comparisons between the inductive and ultrasonic WPT techniques based on maximum range, maximum output power, frequencies and maximum efficiencies are given in Section III. From this information, the inductive WPT tech-

TABLE 2. Existing ultrasonic WPT works.

Reference	Frequency	Medium	Transducer	Range	Efficiency	Output power	Device Size
Kawanabe et al. [52]	1MHz	skin	Piezo electric ceramics	30mm	20	Not specified	Not specified
Suzuki et al. [53]	1MHz	skin	PZT	40mm	20	2.1W	30mm^2
Suzuki et al. [54]	100 kHz	Not specified	piezo	40mm	36	5.4 W	87x134x20 mm^3
Shih and Shih [57]	35kHz	skin	Piezo electric ceramics	70mm	Not specified	1.23mW	$10 \times 10 \times 5.5$ mm^3
Denisov and Yeatman [96]	>1MHz	Tissue	Not specified	10mm	39	Not specified	Not specified
Ozeri and Shmilovitz [58]	673kHz	water	PZT	40mm	27	1W	9.75mm^2
Ozeri et al. [59]	650kHz	Soft-tissues	Piezo-electric	5mm	39.1	100mW	137.44mm^2
Shigeta et al. [61]	1.2MHz	Water	Piezo-electric	Not specified	50	Not specified	41.36mm^2
Maleki et al. [60]	2.3MHz	Tissue	Piezo-ceramic	30–400mm	Not specified	$\approx300\mu W$	$1.2 \times 1.3 \times 8$mm^3
Larson and Towe [62]	1MHz	Nerve	PZT	120mm	Not specified	23mW	41.36mm2
Sanni et al. [64]	200kHz	Air	PZT	70mm	1	8mW	Not specified
Leadbetter et al. [68]	1.07MHz	Skin	PMN-PT composite	Not specified	45	Not specified	12x5mm^2
Lee et al. [66]	250KHz	Tissue & Water	composite type piezo-electric	23mm	21	2.6mW	Not specified
Kim et al. [1]	>350kHz	Bladder	piezo-electric	150mm	Not specified	16µW	40x8mm^2
Mazzilli et al. [69]	1MHz	Water	piezo-electric	105mm	1.6	28mW	5x10mm^2
Lee et al. [97]	280kHz	skin tissue	piezo-electric	18mm	18	2.6mW	122.5mm^2
Fang et al. [72]	3.4MHz	Tissue	PZT	100mm	Not specified	1µW	1.1cm^2
Song et al. [73]	1.15 and 2.3MHz	soft-tissue & air	piezo-electric	20cm	0.4, 1.7 and 2.7	2.48, 8.7, and 12.0 mW	Not specified
Mazzilli et al. [74]	1 MHz	skin	piezo-electric	Not specified	Not specified	184 µW	Not specified
Rosa and Yang [75]	400 kHz	Tissues	piezo-electric	3cm	Not specified	Not specified	Not specified
Vihvelin et al. [76]	1 MHz	Tissue	PMN-PT	3-7mm	25	Not specified	Not specified
Chang et al. [77]	1 MHz	Tissue	PMN-PT	8.5cm	Not specified	100µW	30.5 mm^3
Meng and Kiani [98]	1.8 MHz	Tissue	piezo-electric	3cm	2.11	Not specified	1 mm^3
Charthad et al. [99]	30MHz	Body	piezo-electric	<100mm	Not specified	100µW	4×7.8mm^2

TABLE 3. Comparison of inductive and ultrasonic WPT techniques.

WPT Type	Frequency (min-max)	Active range (max)	Efficiency % (max)	Power (max)
Inductive	2kHz-460MHz	13.5cm	76	15.9W
Ultrasonic	35 kHz-30 MHz	40cm	45	5.4W

nique can provide higher efficiencies with lower distances compared to the ultrasound WPT technique.

The enhancement of the ultrasonic and inductive WPT frameworks demonstrates that there are three noteworthy factors influencing general PTE's: frequency of operation, receiver's diameter and separation between Tx and Rx. This makes the correlation of the two frameworks sensible and practically autonomous of other geometric constraints [96].

V. CONCLUSION

Implantable devices are currently being utilized for health diagnosis as well as treatment applications. Some drawbacks of these devices include the static energy-density, short life span, and large size of batteries utilized for powering these devices. Efforts to decrease the overall size of the implants and reduce the maintenance requirements have focussed on technologies to eliminate the need for batteries. Wireless power transfer methods are being developed to harvest energy

from a remote energy source to power the implants. Devices driven by wireless energy harvesters have unlimited operational duration and offer ease of use and maintenance. Wireless power strategies scale down the size of devices. In this paper, a review of inductive and ultrasonic techniques to wirelessly transfer power to implantable devices was discussed, analyzed. Inductive links are well suited for implantable devices because they transfer energy and bidirectional communication between the internal sensors and the external control devices. Moreover, their small dimensions make them compatible with low-invasive body implantations. However, inductive devices can only be used for shorter communication distances and their efficiency reduces significantly due to misalignment between Tx and Rx coils. For effective WPT to miniaturized implantable devices, the ultrasonic approach has attracted attention due to its very low ultrasonic loss in tissue, low frequency operation, and greater safety when operating in tissues.

ACKNOWLEDGMENT

REFERENCES

[1] A. Kim, C. R. Powell, and B. Ziaie, "An implantable pressure sensing system with electromechanical interrogation scheme," *IEEE Trans. Biomed. Eng.*, vol. 61, no. 7, pp. 2209–2217, Jul. 2014.

[2] T. Campi, S. Cruciani, M. Feliziani, and A. Hirata, "Wireless power transfer system applied to an active implantable medical device," presented at the IEEE Wireless Power Transf. Conf., Jeju, South Korea, May 2014. [Online]. Available: http://ieeexplore.ieee.org/stamp/stamp.jsp?tp=&arnumber=6839612&isnumber=6839547

[3] H. Dinis, I. Colmiais, and P. M. Mendes, "Extending the limits of wireless power transfer to miniaturized implantable electronic devices," *Micromachines*, vol. 8, no. 12, p. 359, 2017.

[4] M. A. Hannan, S. Mutashar, S. A. Samad, and A. Hussain, "Energy harvesting for the implantable biomedical devices: Issues and challenges," *BioMed. Eng. OnLine*, vol. 13, no. 1, p. 79, 2014.

[5] J. Olivo, S. Carrara, and G. De Micheli, "Energy harvesting and remote powering for implantable biosensors," *IEEE Sensors J.*, vol. 11, no. 7, pp. 1573–1586, Jul. 2011.

[6] G. Park, T. Rosing, M. D. Todd, C. R. Farrar, and W. Hodgkiss, "Energy harvesting for structural health monitoring sensor networks," *J. Infrastruct. Syst.*, vol. 14, no. 1, pp. 64–79, 2008.

[7] M. K. Hosain, A. Z. Kouzani, S. J. Tye, O. A. Abulseoud, and M. Berk, "Design and analysis of an antenna for wireless energy harvesting in a head-mountable DBS device," presented at the IEEE 35th Annu. Int. Conf. Eng. Med. Biol. Soc. (EMBC), Osaka, Japan, 2013. [Online]. Available: http://ieeexplore.ieee.org/stamp/stamp.jsp?tp=&arnumber=6610191&isnumber=6609410

[8] K. Agarwal, R. Jegadeesan, Y. Guo, and N. Thakor, "Wireless power transfer strategies for implantable bioelectronics," *IEEE Rev. Biomed. Eng.*, vol. 10, pp. 136–161, 2017.

[9] N. S. Shenck and J. A. Paradiso, "Energy scavenging with shoe-mounted piezoelectrics," *IEEE Micro*, vol. 21, no. 3, pp. 30–42, May/Jun. 2001.

[10] A. Cadei, A. Dionisi, E. Sardini, and M. Serpelloni, "Kinetic and thermal energy harvesters for implantable medical devices and biomedical autonomous sensors," *Meas. Sci. Technol.*, vol. 25, no. 1, p. 012003, 2014.

[11] I. Stark and M. Stordeur, "New micro thermoelectric devices based on bismuth telluride-type thin solid films," in *Proc. 18th Int. Conf. Thermoelectr. (ICT)*, Baltimore, MD, USA, 1999, pp. 465–472.

[12] M. Strasser, R. Aigner, C. Lauterbach, T. F. Sturm, M. Franosh, and G. Wachutka, "Micromachined CMOS thermoelectric generators as on-chip power supply," presented at the 12th Int. Conf. Solid-State Sens., Actuators Microsyst. Dig. Tech. Papers, Boston, MA, USA, 2003. [Online]. Available: http://ieeexplore.ieee.org/stamp/stamp.jsp?tp=&arnumber=1215249&isnumber=27333

[13] A. Cadei, A. Dionisi, E. Sardini, and M. Serpelloni, "Kinetic and thermal energy harvesters for implantable medical devices and biomedical autonomous sensors," *Meas. Sci. Technol.*, vol. 25, no. 1, p. 012003, Nov. 2013.

[14] Z. Chen, M.-K. Law, P.-I. Mak, and R. P. Martins, "A single-chip solar energy harvesting IC using integrated photodiodes for biomedical implant applications," *IEEE Trans. Biomed. Circuits Syst.*, vol. 11, no. 1, pp. 44–53, Feb. 2017.

[15] P. D. Mitcheson, "Energy harvesting for human wearable and implantable bio-sensors," presented at the IEEE Annu. Int. Conf. Eng. Med. Biol., Buenos Aires, Argentina, 2010. [Online]. Available: http://ieeexplore.ieee.org/stamp/stamp.jsp?tp=&arnumber=5627952&isnumber=5625939

[16] E. Moon, D. Blaauw, and J. D. Phillips, "Subcutaneous photovoltaic infrared energy harvesting for bio-implantable devices," *IEEE Trans. Electron Devices*, vol. 64, no. 5, pp. 2432–2437, May 2017.

[17] V. B. Gore and D. H. Gawali, "Wireless power transfer technology for medical applications," presented at the Conf. Adv. Signal Process. (CASP), Pune, India, Jun. 2016. [Online]. Available: http://ieeexplore.ieee.org/stamp/stamp.jsp?tp=&arnumber=7746214&isnumber=7746126

[18] A. L. Benabid, S. Chabardes, J. Mitrofanis, and P. Pollak, "Deep brain stimulation of the subthalamic nucleus for the treatment of Parkinson's disease," *Lancet Neurol.*, vol. 8, no. 1, pp. 67–81, Jan. 2009.

[19] R. G. Hauser, W. T. Katsiyiannis, C. C. Gornick, A. K. Almquist, and L. M. Kallinen, "Deaths and cardiovascular injuries due to device-assisted implantable cardioverter-defibrillator and pacemaker lead extraction," *Europace*, vol. 12, no. 3, pp. 395–401, Mar. 2010.

[20] R. Bashirullah, "Wireless implants," *IEEE Microw. Mag.*, vol. 11, no. 7, pp. S14–S23, Dec. 2010.

[21] X. Mou and H. Sun, "Wireless power transfer: Survey and roadmap," presented at the IEEE 81st Veh. Technol. Conf. (VTC Spring), Glasgow, U.K., 2015. [Online]. Available: http://ieeexplore.ieee.org/stamp/stamp.jsp?tp=&arnumber=7146165&isnumber=7145573

[22] R. Jegadeesan, K. Agarwal, Y.-X. Guo, S.-C. Yen, and N. V. Thakor, "Wireless power delivery to flexible subcutaneous implants using capacitive coupling," *IEEE Trans. Microw. Theory Techn.*, vol. 65, no. 1, pp. 280–292, Jan. 2017.

[23] M. R. Awal, M. Jusoh, T. Sabapathy, M. R. Kamarudin, and R. A. Rahim, "State-of-the-art developments of acoustic energy transfer," *Int. J. Antennas Propag.*, vol. 2016, Jul. 2016, Art. no. 3072528, doi: 10.1155/2016/3072528.

[24] S. Raju, R. Wu, M. Chan, and C. P. Yue, "Modeling of mutual coupling between planar inductors in wireless power applications," *IEEE Trans. Power Electron.*, vol. 29, no. 1, pp. 481–490, Jan. 2014.

[25] P. R. Troyk and G. A. DeMichele, "Inductively-coupled power and data link for neural prostheses using a class-E oscillator and FSK modulation," in *Proc. 25th Annu. Int. Conf. Eng. Med. Biol. Soc.*, Cancun, Mexico, vol. 4, Sep. 2003, pp. 3376–3379.

[26] Y. Hu and M. Sawan, "A fully integrated low-power BPSK demodulator for implantable medical devices," *IEEE Trans. Circuits Syst. I, Reg. Papers*, vol. 52, no. 12, pp. 2552–2562, Dec. 2005.

[27] G. Wang, W. Liu, M. Sivaprakasam, M. Zhou, J. D. Weiland, and M. S. Humayun, "A dual band wireless power and data telemetry for retinal prosthesis," presented at the Int. Conf. Eng. Med. Biol. Soc., New York, NY, USA, 2006. [Online]. Available: http://ieeexplore.ieee.org/stamp/stamp.jsp?tp=&arnumber=4462775&isnumber=4461641

[28] M. Ghovanloo and S. Atluri, "A wide-band power-efficient inductive wireless link for implantable microelectronic devices using multiple carriers," *IEEE Trans. Circuits Syst. I, Reg. Papers*, vol. 54, no. 10, pp. 2211–2221, Oct. 2007.

[29] Z. Lu and M. Sawan, "An 8 Mbps data rate transmission by inductive link dedicated to implantable devices," presented at the IEEE Int. Symp. Circuits Syst., Seattle, WA, USA, May 2008. [Online]. Available: http://ieeexplore.ieee.org/stamp/stamp.jsp?tp=&arnumber=4542103&isnumber=4541329

[30] S. Mandal and R. Sarpeshkar, "Power-efficient impedance-modulation wireless data links for biomedical implants," *IEEE Trans. Biomed. Circuits Syst.*, vol. 2, no. 4, pp. 301–315, Dec. 2008.

[31] H. Ali, T. J. Ahmad, and S. A. Khan, "Inductive link design for medical implants," presented at the IEEE Symp. Ind. Electron. Appl., Kuala Lumpur, Malaysia, Oct. 2009. [Online]. Available: http://ieeexplore.ieee.org/stamp/stamp.jsp?tp=&arnumber=5356376&isnumber=5356300

[32] K. M. Silay, C. Dehollain, and M. Declercq, "Inductive power link for a wireless cortical implant with biocompatible packaging," presented at the IEEE SENSORS, Kona, HI, USA, 2010. [Online]. Available: http://ieeexplore.ieee.org/stamp/stamp.jsp?tp=&arnumber=5690844&isnumber=5689839

[33] R. Carta, J. Thoné, G. Gosset, D. Flandre, and R. Puers, "A self-tuning inductive powering system for biomedical implants," *Procedia Eng.*, vol. 25, pp. 1585–1588, Sep. 2011, doi: 10.1016/j.proeng.2011.12.392.

[34] M. Kiani, U.-M. Jow, and M. Ghovanloo, "Design and optimization of a 3-coil inductive link for efficient wireless power transmission," *IEEE Trans. Biomed. Circuits Syst.*, vol. 5, no. 6, pp. 579–591, Dec. 2011.

[35] A. K. Ram Rakhyani, S. Mirabbasi, and M. Chiao, "Design and optimization of resonance-based efficient wireless power delivery systems for biomedical implants," *IEEE Trans. Biomed. Circuits Syst.*, vol. 5, no. 1, pp. 48–63, Feb. 2011.

[36] K. M. Silay, C. Dehollain, and M. Declercq, "Inductive power link for a wireless cortical implant with two-body packaging," *IEEE Sensors J.*, vol. 11, no. 11, pp. 2825–2833, Nov. 2011.

[37] Z. Duan and Y.-X. Guo, "Rectangular coils modeling for inductive links in implantable biomedical devices," presented at the IEEE Int. Symp. Antennas Propag. (APSURSI), Spokane, WA, USA, 2011. [Online]. Available: http://ieeexplore.ieee.org/stamp/stamp.jsp?tp=&arnumber=5996725&isnumber=5996365

[38] M. Kiani and M. Ghovanloo, "A figure-of-merit for design of high performance inductive power transmission links for implantable microelectronic devices," in *Proc. IEEE 34th Annu. Int. Conf. EMBS*, Aug./Sep. 2012, pp. 847–850.

[39] K. M. Silay, C. Dehollain, and M. Declercq, "A closed-loop remote powering link for wireless cortical implants," *IEEE Sensors J.*, vol. 13, no. 9, pp. 3226–3235, Sep. 2013.

[40] K. Keikhosravy, P. Kamalinejad, S. Mirabbasi, K. Takahata, and V. C. M. Leung, "An ultra-low-power monitoring system for inductively coupled biomedical implants," presented at the IEEE Int. Symp. Circuits Syst. (ISCAS), Beijing, China, 2013. [Online]. Available: http://ieeexplore.ieee.org/stamp/stamp.jsp?tp=&arnumber=6572333&isnumber=6571764

[41] A. K. RamRakhyani and G. Lazzi, "On the design of efficient multi-coil telemetry system for biomedical implants," *IEEE Trans. Biomed. Circuits Syst.*, vol. 7, no. 1, pp. 11–23, Feb. 2013.

[42] E. G. Kilinc *et al.*, "Remotely powered implantable heart monitoring system for freely moving animals," presented at the IEEE 5th Int. Workshop Adv. Sensors Interfaces. (IWASI), Bari, Italy, 2013.

[43] S. A. Mirbozorgi, H. Bahrami, M. Sawan, and B. Gosselin, "A smart multicoil inductively coupled array for wireless power transmission," *IEEE Trans. Ind. Electron.*, vol. 61, no. 11, pp. 6061–6070, Nov. 2014.

[44] G. M. Kava, S. L. Patil, and U. M. Chaskar, "Efficiency improvement of two coil wireless power transfer system for biomedical implants," presented at the Int. Conf. Ind. Instrum. Control (ICIC), Pune, India, 2015. [Online]. Available: http://ieeexplore.ieee.org/stamp/stamp.jsp?tp=&arnumber=7150952&isnumber=7150576

[45] H. Kassiri *et al.*, "Inductively-powered direct-coupled 64-channel chopper-stabilized epilepsy-responsive neurostimulator with digital offset cancellation and tri-band radio," presented at the 40th Eur. Solid State Circuits Conf. (ESSCIRC), Venice Lido, Italy, 2014. [Online]. Available: http://ieeexplore.ieee.org/stamp/stamp.jsp?tp=&arnumber=6942030&isnumber=6941994

[46] Q. Xu, D. Hu, B. Duan, and J. He, "A fully implantable stimulator with wireless power and data transmission for experimental investigation of epidural spinal cord stimulation," *IEEE Trans. Neural Syst. Rehabil. Eng.*, vol. 23, no. 4, pp. 683–692, Jul. 2015.

[47] V. Valente, C. Eder, N. Donaldson, and A. Demosthenous, "A high-power CMOS class-D amplifier for inductive-link medical transmitters," *IEEE Trans. Power Electron.*, vol. 30, no. 8, pp. 4477–4488, Aug. 2015.

[48] A. Ibrahim and M. Kiani, "Inductive power transmission to millimeter-sized biomedical implants using printed spiral coils," presented at the IEEE 38th Annu. Int. Conf. Eng. Med. Biol. Soc. (EMBC), Orlando, FL, USA, Aug. 2016. [Online]. Available: http://ieeexplore.ieee.org/stamp/stamp.jsp?tp=&arnumber=7591801&isnumber=7590615

[49] N. Soltani, M. S. Aliroteh, M. T. Salam, J. L. P. Velazquez, and R. Genov, "Low-radiation cellular inductive powering of rodent wireless brain interfaces: Methodology and design guide," *IEEE Trans. Biomed. Circuits Syst.*, vol. 10, no. 4, pp. 920–932, Aug. 2016.

[50] M. P. Kazmierkowski, R. M. Miskiewicz, and A. J. Moradewicz, "Inductive coupled contactless energy transfer systems—A review," presented at the Sel. Problems Elect. Eng. Electron. (WZEE), Kielce, Poland, Sep. 2015. [Online]. Available: http://ieeexplore.ieee.org/stamp/stamp.jsp?tp=&isnumber=7394003

[51] B. Zhao, N.-C. Kuo, and A. M. Niknejad, "A gain boosting array technique for weakly-coupled wireless power transfer," *IEEE Trans. Power Electron.*, vol. 32, no. 9, pp. 7130–7139, Sep. 2017.

[52] H. Kawanabe, T. Katane, H. Saotome, O. Saito, and K. Kobayashi, "Power and information transmission to implanted medical device using ultrasonic," *Jpn. J. Appl. Phys.*, vol. 40, no. 5B, p. 3865, 2001.

[53] S.-N. Suzuki, S. Kimura, T. Katane, H. Saotome, O. Saito, and K. Kobayashi, "Power and interactive information transmission to implanted medical device using ultrasonic," *Jpn. J. Appl. Phys.*, vol. 41, no. 5B, Jan. 2002.

[54] S. N. Suzuki, T. Katane, and O. Saito, "Fundamental study of an electric power transmission system for implanted medical devices using magnetic and ultrasonic energy," *J. Artif. Organs*, vol. 6, no. 2, pp. 145–148, 2003.

[55] S. Arra, J. Leskinen, J. Heikkila, and J. Vanhala, "Ultrasonic power and data link for wireless implantable applications," presented at the 2nd Int. Symp. Wireless Pervasive Comput., San Juan, Puerto Rico, Feb. 2007. [Online]. Available: http://ieeexplore.ieee.org/stamp/stamp.jsp?tp=&arnumber=4147127&isnumber=4139316

[56] Y. Shigeta, T. Yamamoto, K. Fujimori, M. Sanagi, S. Nogi, and T. Tsukagoshi, "Development of ultrasonic wireless power transmission system for implantable electronic devices," in *Proc. 2nd Eur. Wireless Technol. Conf.*, Rome, Italy, Sep. 2009, pp. 49–52.

[57] P.-J. Shih and W.-P. Shih, "Design, fabrication, and application of bio-implantable acoustic power transmission," *J. Microelectromech. Syst.*, vol. 19, no. 3, pp. 494–502, Jun. 2010.

[58] S. Ozeri and D. Shmilovitz, "Ultrasonic transcutaneous energy transfer for powering implanted devices," *Ultrasonics*, vol. 50, no. 6, pp. 556–566, May 2010.

[59] S. Ozeri, D. Shmilovitz, S. Singer, and C.-C. Wang, "Ultrasonic transcutaneous energy transfer using a continuous wave 650 kHz Gaussian shaded transmitter," *Ultrasonics*, vol. 50, no. 7, pp. 666–674, Jun. 2010.

[60] T. Maleki, N. Cao, S. H. Song, C. Kao, S.-C. Ko, and B. Ziaie, "An ultrasonically powered implantable micro-oxygen generator (IMOG)," *IEEE Trans. Biomed. Eng.*, vol. 58, no. 11, pp. 3104–3111, Nov. 2011.

[61] Y. Shigeta, Y. Hori, K. Fujimori, K. Tsuruta, and S. Nogi, "Development of highly efficient transducer for wireless power transmission system by ultrasonic," presented at the IEEE MTT-S Int. Microw. Workshop Ser. Innov. Wireless Power Transmiss., Technol., Syst., Appl., Kyoto, Japan, May 2011. [Online]. Available: http://ieeexplore.ieee.org/stamp/stamp.jsp?tp=&arnumber=5877115&isnumber=5876647

[62] P. J. Larson and B. C. Towe, "Miniature ultrasonically powered wireless nerve cuff stimulator," in *Proc. 5th IEEE/EMBS Int. Conf. Neural Eng. (NER)*, Cancun, Mexico, Apr./May 2011, pp. 265–268.

[63] J.-Y. Tsai, K.-H. Huang, J.-R. Wang, S.-I. Liu, and P.-C. Li, "Ultrasonic wireless power and data communication for neural stimulation," presented at the IEEE Int. Ultrason. Symp., Orlando, FL, USA, Oct. 2011. [Online]. Available: http://ieeexplore.ieee.org/stamp/stamp.jsp?tp=&arnumber=6293708&isnumber=6293047

[64] A. Sanni, A. Vilches, and C. Toumazou, "Inductive and ultrasonic multi-tier interface for low-power, deeply implantable medical devices," *IEEE Trans. Biomed. Circuits Syst.*, vol. 6, no. 4, pp. 297–308, Aug. 2012.

[65] F. Mazzilli, P. E. Thoppay, V. Praplan, and C. Dehollain, "Ultrasound energy harvesting system for deep implanted-medical-devices (IMDs)," presented at the IEEE Int. Symp. Circuits Syst., Seoul, South Korea, May 2012. [Online]. Available: http://ieeexplore.ieee.org/stamp/stamp.jsp?tp=&arnumber=6271911&isnumber=6270389

[66] S. Q. Lee, W. Youm, and G. Hwang, "Biocompatible wireless power transferring based on ultrasonic resonance devices," in *Proc. Meetings Acoust.*, vol. 19, no. 1, 2013, p. 030030.

[67] S. Banerji, W. L. Goh, J. H. Cheong, and M. Je, "CMUT ultrasonic power link front-end for wireless power transfer deep in body," presented at the IEEE MTT-S Int. Microw. Workshop Ser. RF Wireless Technol. Biomed. Healthcare Appl. (IMWS-BIO), Dec. 2013.

[68] J. Leadbetter, J. Brown, and R. Adamson, "The design of ultrasonic lead magnesium niobate-lead titanate composite transducers for power and signal delivery to implanted hearing aids," *J. Acoust. Soc. Amer.*, vol. 133, no. 5, p. 3268, May 2013.

[69] F. Mazzilli, C. Lafon, and C. Dehollain, "A 10.5 cm ultrasound link for deep implanted medical devices," *IEEE Trans. Biomed. Circuits Syst.*, vol. 8, no. 5, pp. 738–750, Oct. 2014.

[70] Q. S. Lee, W. Youm, G. Hwang, S. K. Moon, and Y. Ozturk, "Resonant ultrasonic wireless power transmission for bio-implants," *Act. Passive Smart Struct. Integr. Syst.*, vol. 9057, p. 90570J, Mar. 2014, doi: 10.1117/12.2046600.

[71] D. Shmilovitz, S. Ozeri, C.-C. Wang, and B. Spivak, "Noninvasive control of the power transferred to an implanted device by an ultrasonic transcutaneous energy transfer link," *IEEE Trans. Biomed. Eng.*, vol. 61, no. 4, pp. 995–1004, Apr. 2014.

[72] B. Fang, T. Feng, M. Zhang, and S. Chakrabartty, "Feasibility of B-mode diagnostic ultrasonic energy transfer and telemetry to a cm^2 sized deep-tissue implant," presented at the IEEE Int. Symp. Circuits Syst. (ISCAS), Lisbon, Portugal, May 2015. [Online]. Available: http://ieeexplore.ieee.org/stamp/stamp.jsp?tp=&arnumber=7168750&isnumber=7168553

[73] S. H. Song, A. Kim, and B. Ziaie, "Omnidirectional ultrasonic powering for millimeter-scale implantable devices," *IEEE Trans. Biomed. Eng.*, vol. 62, no. 11, pp. 2717–2723, Nov. 2015.

[74] F. Mazzilli and C. Dehollain, "184 μW ultrasonic on–off keying/amplitude-shift keying demodulator for downlink communication in deep implanted medical devices," *Electron. Lett.*, vol. 52, no. 7, pp. 502–504, 2016.

[75] B. M. G. Rosa and G. Z. Yang, "Active implantable sensor powered by ultrasounds with application in the monitoring of physiological parameters for soft tissues," presented at the IEEE 13th Int. Conf. Wearable Implant. Body Sensor Netw. (BSN), San Francisco, CA, USA, Jun. 2016. [Online]. Available: http://ieeexplore.ieee.org/stamp/stamp.jsp?tp=&arnumber=7516281&isnumber=7516211

[76] H. Vihvelin, J. R. Leadbetter, M. Bance, J. A. Brown, and R. B. A. Adamson, "Compensating for tissue changes in an ultrasonic power link for implanted medical devices," *IEEE Trans. Biomed. Circuits Syst.*, vol. 10, no. 2, pp. 404–411, Apr. 2016.

[77] T. C. Chang, M. L. Wang, J. Charthad, M. J. Weber, and A. Arbabian, "A 30.5 mm^3 fully packaged implantable device with duplex ultrasonic data and power links achieving 95 kb/s with <10^{-4} BER at 8.5 cm depth," in *IEEE Int. Solid-State Circuits Conf. (ISSCC) Dig. Tech. Papers*, San Francisco, CA, USA, Feb. 2017, pp. 460–461. [Online]. Available: http://ieeexplore.ieee.org/stamp/stamp.jsp?tp=&arnumber=7870460&isnumber=7870233

[78] M. Meng and M. Kiani, "Design and optimization of ultrasonic wireless power transmission links for millimeter-sized biomedical implants," *IEEE Trans. Biomed. Circuit Syst.*, vol. 11, no. 1, pp. 98–107, Feb. 2017.

[79] R. Cartaa *et al.*, "Design and implementation of advanced systems in a flexible-stretchable technology for biomedical applications," *Sens. Actuators A, Phys.*, vol. 156, no. 1, pp. 79–87, Nov. 2009.

[80] Z. N. Low, R. A. Chinga, R. Tseng, and J. Lin, "Design and test of a high-power high-efficiency loosely coupled planar wireless power transfer system," *IEEE Trans. Ind. Electron.*, vol. 56, no. 5, pp. 1801–1812, May 2009.

[81] Y. Yu, H. Hao, W. Wang, and L. Li, "Simulative and experimental research on wireless power transmission technique in implantable medical device," presented at the IEEE Annu. Int. Conf. Eng. Med. Biol. Soc., Minneapolis, MN, USA, Sep. 2009. [Online]. Available: http://ieeexplore.ieee.org/stamp/stamp.jsp?tp=&arnumber=5332831&isnumber=5332379

[82] G. Simard, M. Sawan, and D. Massicotte, "High-speed OQPSK and efficient power transfer through inductive link for biomedical implants," *IEEE Trans. Biomed. Circuits Syst.*, vol. 4, no. 3, pp. 192–200, Jun. 2010.

[83] K. M. Silay, C. Dehollain, and M. Declercq, "Inductive power link for a wireless cortical implant with biocompatible packaging," presented at the IEEE SENSORS, Sep. 2010.

[84] M. A. Adeeb, A. B. Islam, M. R. Haider, F. S. Tulip, M. N. Ericson, and S. K. Islam, "An inductive link-based wireless power transfer system for biomedical applications," *Act. Passive Electron. Compon.*, vol. 2012, Mar. 2012, Art. no. 879294, doi: 10.1155/2012/879294.

[85] E. G. Kilinc, M. A. Ghanad, F. Maloberti, and C. Dehollain, "Short range remote powering of implanted electronics for freely moving animals," presented at the IEEE 11th Int. New Circuits Syst. Conf. (NEWCAS), Paris, France, Jun. 2013.

[86] E. G. Kilinc, C. Dehollain, and F. Maloberti, "A low-power PPM demodulator for remotely powered batteryless implantable devices," presented at the IEEE 57th Int. Midwest Symp. Circuits Syst. (MWSCAS), College Station, TX, USA, Aug. 2014.

[87] M. Kiani, B. Lee, P. Yeon, and M. Ghovanloo, "A Q-modulation technique for efficient inductive power transmission," *IEEE J. Solid-State Circuits*, vol. 50, no. 12, pp. 2839–2848, Dec. 2015.

[88] M. Zargham and P. G. Gulak, "Fully integrated on-chip coil in 0.13 μm CMOS for wireless power transfer through biological media," *IEEE Trans. Biomed. Circuits Syst.*, vol. 9, no. 2, pp. 259–271, Apr. 2015.

[89] A. Ibrahim and M. Kiani, "A figure-of-merit for design and optimization of inductive power transmission links for millimeter-sized biomedical implants," *IEEE Trans. Biomed. Circuits Syst.*, vol. 10, no. 6, pp. 1100–1111, Dec. 2016.

[90] D. Ahn and M. Ghovanloo, "Optimal design of wireless power transmission links for millimeter-sized biomedical implants," *IEEE Trans. Biomed. Circuits Syst.*, vol. 10, no. 1, pp. 125–137, Feb. 2016.

[91] H. S. Gougheri and M. Kiani, "Optimal frequency for powering millimeter-sized biomedical implants inside an inductively-powered homecage," presented at the IEEE 38th Annu. Int. Conf. Eng. Med. Biol. Soc., Aug. 2016.

[92] H. S. Gougheri and M. Kiani, "Optimal wireless receiver structure for omnidirectional inductive power transmission to biomedical implants," presented at the IEEE 38th Annu. Int. Conf. Eng. Med. Biol. Soc. (EMBC), Orlando, FL, USA, Aug. 2016.

[93] H. S. Gougheri and M. Kiani, "Adaptive reconfigurable voltage/current-mode power management with self-regulation for extended-range inductive power transmission," in *IEEE Int. Solid-State Circuits Conf. (ISSCC) Dig. Tech. Papers*, San Francisco, CA, USA, Feb. 2017, pp. 374–375.

[94] J. Pan, A. A. Abidi, D. Rozgić, H. Chandrakumar, and D. Marković, "An inductively-coupled wireless power-transfer system that is immune to distance and load variations," in *IEEE Int. Solid-State Circuits Conf. (ISSCC) Dig. Tech. Papers*, San Francisco, CA, USA, Feb. 2017, pp. 382–383.

[95] D. Jiang, D. Cirmirakis, M. Schormans, T. A. Perkins, N. Donaldson, and A. Demosthenous, "An integrated passive phase-shift keying modulator for biomedical implants with power telemetry over a single inductive link," *IEEE Trans. Biomed. Circuits Syst.*, vol. 11, no. 1, pp. 64–77, Feb. 2017.

[96] A. Denisov and E. Yeatman, "Ultrasonic vs. inductive power delivery for miniature biomedical implants," presented at the Int. Conf. Body Sensor Netw., Singapore, Jun. 2010, pp. 84–89.

[97] S. Q. Lee, W. Youm, G. Hwang, and K. S. Moon, "Wireless power transferring and charging for implantable medical devices based on ultrasonic resonance," in *Proc. 22nd Int. Congr. Sound Viberation*, 2015, pp. 1–7.

[98] M. Meng and M. Kiani, "Design and optimization of ultrasonic wireless power transmission links for millimeter-sized biomedical implants," *IEEE Trans. Biomed. Circuit Syst.*, vol. 11, no. 1, pp. 98–107, Feb. 2017.

[99] J. Charthad, M. J. Weber, T. C. Chang, and A. Arbabian, "A mm-sized implantable medical device (IMD) with ultrasonic power transfer and a hybrid bi-directional data link," *IEEE J. Solid-State Circuits*, vol. 50, no. 8, pp. 1741–1753, Aug. 2015.

RAJESH V. TAALLA is currently pursuing the Ph.D. degree with the School of Engineering, Deakin University, Australia. His current research interest includes wireless power transfer devices for medical implants.

MD. SHAMSUL AREFIN received the Ph.D. degree from Monash University, Australia. He is currently a Postdoctoral Research Fellow with the School of Engineering, Deakin University, Australia. His current research interests include analog circuit and chip design for medical devices.

AKIF KAYNAK received the B.Sc. degree from The University of Manchester, U.K., the M.Sc. degree from the Rutgers State University of New Jersey, USA, and the Ph.D. degree from the University of Technology, Sydney. After receiving the Ph.D. degree in 1994, he was a Lecturer with the Department of Engineering Sciences, Middle East Technical University and then a Research Fellow with the Queensland University of Technology. He joined Deakin University, in 2001, where he is currently an Associate Professor in mechanical engineering. His research interests include polymer coatings, functional textiles, and sensors.

ABBAS Z. KOUZANI (M'95) received the B.Sc. degree in computer engineering from the Sharif University of Technology, Iran, the M.Sc. degree in electrical and electronics engineering from The University of Adelaide, and the Ph.D. degree in electrical and electronics engineering from Flinders University, Australia. He was a Lecturer with the School of Engineering, Deakin University, and a Senior Lecturer with the School of Electrical Engineering and Computer Science, The University of Newcastle, Australia. He was the Associate Head of School (Research) with the School of Engineering, Deakin University, for several years. He is currently a Professor with the School of Engineering, Deakin University. He is also the Director of the Deakin University's Advanced Integrated Microsystems Research Group. He has carried out applied research and consultancy for over 25 Australian and international companies. He received about $15 million research grants. He has published over 330 papers. His current research interests include medical/biological microsystems, microfluidic lab-on-a-chip devices, bioinstruments, biosensors, and implants. He is an Oz Reader with the Australian Research Council.

• • •